SIMULATIONS of HIGH betaN*H ADVANCED TOKAMAK DISCHARGES IN DIII-D WITH THE 3D NONLINEAR CODE NFTC .

A.M.Popov, N.N.Popova
Moscow State University

V.S.Chan,R.J. La Haye, A.D.Turnbull
General Atomics

M.Murakami
Oak Ridge National Laboratory

APS meeting, Quebec Canada ,23-27 October 2000

ABSTRACT

Nonlinear self-consistent MHD stability simulations of neoclassical tearing modes (NTM) in high betaN Advanced Tokamak (AT) are presented. Radially localized electron cyclotron current drive (ECCD) current profile control is considered based on DIII-D discharge # 99411 in which $\beta_N = 3.9$ and H89P-factor=2.9 are reached. Simulations were performed with the full 3D nonlinear code NFTC. Neoclassical terms are included in the basic equations for the magnetic field and pressure. An effective fully implicit numerical scheme allows the transport profile to evolve self-consistently with the nonlinear MHD instabilities and an externally applied source such as ECCD. NTM activity with m/n=2/1 is found in simulations to correspond to experiment. It is shown that magnetic islands can be quickly suppressed by localized ECCD at q=2 before the mode grows substantially. The time response and nonlinear evolution of the 2/1 island width for ECCD and required modulation phasing, the CD location with respect to the q=2 surface, and the width of the spatial distribution are determined. The possibility of q-profile modification by ECCD well before MHD activity to keep $q_{min} > 2$, so that the discharge evolves stably is also discussed.

GOAL

- Simulations of the nonlinear MHD stability of high β_N AT discharge in DIII-D by three-dimensional MHD code NFTC.
  -Discharge # 99411 at the moment t=1800ms ($q_{min} = 1.67$)
  - The problem of critical seed island necessary to triger NTMs.
  - Comparison with experiment.
  -Suppression of NTM instability by radially localized ECCD around q=2.(Magnitude of ECCD, width of driven current, location)

- **Motivation.** Discharges with $q_{min} > 1.5$ and NCS (Negative Central Shear) are the leading scenario for AT (Advanced Tokamak) operation in DIII-D.
  - NTM modes still remain a significant obstacle to approaching the ideal β limit.
  - High β_N ($\beta_N \sim 3$) is oserved in long pulse NCS discharges.No sawteeth or fishbons to provide the seed island.

- The nonlinear three dimensional evolution of a tokamak plasma is described by the full (nonreduced, compressible) MHD system of equations in general toroidal geometry.
- We seek the solutions $\{\mathbf{V}, \mathbf{B}, P\}$ by decomposition:

$$\begin{aligned}
\mathbf{V}(\rho,\theta,\varphi,t) &= \mathbf{V_0}(\rho,\theta) + \underbrace{\hat{\mathbf{V}}(\rho,\theta,t)}_{n=0} + \underbrace{\mathbf{V}(\rho,\theta,\varphi,t)}_{n\neq 0} \\
\mathbf{B}(\rho,\theta,\varphi,t) &= \mathbf{B}_{\rm eq}(\rho,\theta) + \underbrace{\hat{\mathbf{B}}(\rho,\theta,t)}_{n=0} + \underbrace{\mathbf{B}(\rho,\theta,\varphi,t)}_{n\neq 0} \\
P(\rho,\theta,\varphi,t) &= P_{\rm eq}(\rho) + \underbrace{\hat{P}(\rho,\theta,t)}_{n=0} + \underbrace{P(\rho,\theta,\varphi,t)}_{n\neq 0}
\end{aligned}$$

- Our problem is to find $\{\mathbf{V}, \mathbf{B}, P\}$ for a given $\{\mathbf{V}_0, \mathbf{B}_{\rm eq}, P_{\rm eq}\}$.
- The solutions satisfy the fixed boundary conditions:

$$\mathbf{B}_n = 0, \quad \mathbf{V}_n = 0, \quad P = 0.$$

Neoclassical terms in the model are included :

- Helical and axi-symmetric bootstrap current terms are added into the magnetic field equation.
- Polarization current effect is included in the magnetic field equation as a helical current perturbation.
- Radially localized toroidal current density from ECCD is included in the magnetic field equation .
- The equation for pressure is modified by incorporated the perpendicular transport across a seed magnetic island and along magnetic field lines .

$$
\begin{aligned}
\overline{\rho}\frac{\partial \mathbf{V}}{\partial t} &= -\overline{\rho}[(\mathbf{V}_0\cdot\nabla)\mathbf{V}+(\mathbf{V}\cdot\nabla)\mathbf{V}_0]-\beta_0\nabla P+ \\
&+[[\nabla\times\mathbf{B}_{\rm eq}]\times\mathbf{B}]+[[\nabla\times\mathbf{B}]\times\mathbf{B}_{\rm eq}]+\nu\triangle\mathbf{V}- \\
&-\overline{\rho}[(\hat{\mathbf{V}}\cdot\nabla)\mathbf{V}+(\mathbf{V}\cdot\nabla)\hat{\mathbf{V}}]+[[\nabla\times\hat{\mathbf{B}}]\times\mathbf{B}] \\
&+[[\nabla\times\mathbf{B}]\times\hat{\mathbf{B}}]-\overline{\rho}[(\mathbf{V}\cdot\nabla)\mathbf{V}]+[[\nabla\times\mathbf{B}]\times\mathbf{B}]; \qquad (1)\\
\frac{\partial \mathbf{B}}{\partial t} &= [\nabla\times[\mathbf{V}\times\mathbf{B}_{\rm eq}]]+[\nabla\times[\mathbf{V}_0\times\mathbf{B}]]-[\nabla\times(\eta[\nabla\times\mathbf{B}])]+ \\
&+[\nabla\times[\hat{\mathbf{V}}\times\mathbf{B}]]+[\nabla\times[\mathbf{V}\times\hat{\mathbf{B}}]]+ \\
&+[\nabla\times[\mathbf{V}\times\mathbf{B}]]+\underline{\underline{[\nabla\times\mathbf{E}_{\rm P}]}}; \qquad (2)\\
\frac{\partial P}{\partial t} &= -\nabla\cdot(P_{\rm eq}\mathbf{V})-\nabla\cdot(P\mathbf{V}_0)-(\Gamma-1)[P_{\rm eq}(\nabla\cdot\mathbf{V}) \\
&+P(\nabla\cdot\mathbf{V}_0)]-\nabla\cdot(\hat{P}\mathbf{V})-\nabla\cdot(P\hat{\mathbf{V}})-(\Gamma-1)[\hat{P}(\nabla\cdot\mathbf{V}) \\
&+P(\nabla\cdot\hat{\mathbf{V}})]-\nabla\cdot(P\mathbf{V})-(\Gamma-1)[P(\nabla\cdot\mathbf{V})] \\
&+\underline{\nabla_\perp\cdot(\chi_\perp\nabla_\perp P)+\nabla_\parallel\cdot(\chi_\parallel\nabla_\parallel P)}; \qquad (3)
\end{aligned}
$$

$$
\begin{aligned}
\overline{\rho}\frac{\partial \hat{\mathbf{V}}}{\partial t} &= -\overline{\rho}[(\mathbf{V}_0\cdot\nabla)\mathbf{V}_0+(\mathbf{V}_0\cdot\nabla)\hat{\mathbf{V}}+(\hat{\mathbf{V}}\cdot\nabla)\mathbf{V}_0]-\beta_0\nabla\hat{P}+ \\
&+[[\nabla\times\mathbf{B}_{\rm eq}]\times\hat{\mathbf{B}}]+[[\nabla\times\hat{\mathbf{B}}]\times\mathbf{B}_{\rm eq}]+\nu\triangle\hat{\mathbf{V}}- \qquad (4)\\
&-\overline{\rho}(\hat{\mathbf{V}}\cdot\nabla)\hat{\mathbf{V}}+[[\nabla\times\hat{\mathbf{B}}]\times\hat{\mathbf{B}}]+ \\
&+[[\nabla\times\mathbf{B}]\times\mathbf{B}]_{n=0}-\overline{\rho}[(\mathbf{V}\cdot\nabla)\mathbf{V}]_{n=0}; \\
\frac{\partial \hat{\mathbf{B}}}{\partial t} &= [\nabla\times[\hat{\mathbf{V}}\times\mathbf{B}_{\rm eq}]]+[\nabla\times[\mathbf{V}_0\times\hat{\mathbf{B}}]]-[\nabla\times(\eta[\nabla\times\hat{\mathbf{B}}])]+ \\
&+[\nabla\times[\hat{\mathbf{V}}\times\hat{\mathbf{B}}]]+[\nabla\times[\mathbf{V}\times\mathbf{B}]_{n=0}]+\underline{\underline{[\nabla\times\hat{\mathbf{E}}_{\rm P}]}}; \qquad (5)\\
\frac{\partial \hat{P}}{\partial t} &= -\nabla\cdot(P_{\rm eq}\hat{\mathbf{V}})-\nabla\cdot(\hat{P}\mathbf{V}_0)-(\Gamma-1)[P_{\rm eq}(\nabla\cdot\hat{\mathbf{V}}) \\
&+\hat{P}(\nabla\cdot\mathbf{V}_0)]-\nabla\cdot(\hat{P}\hat{\mathbf{V}})-(\Gamma-1)\hat{P}(\nabla\cdot\hat{\mathbf{V}})- \\
&-(\nabla\cdot(P\mathbf{V}))_{n=0}-(\Gamma-1)[P(\nabla\cdot\mathbf{V})]_{n=0} \\
&+\underline{\nabla_\perp\cdot(\chi_\perp\nabla_\perp\hat{P})+\nabla_\parallel\cdot(\chi_\parallel\nabla_\parallel\hat{P})}+Q; \qquad (6)
\end{aligned}
$$

$$
P = f(\overline{\rho},T). \qquad (7)
$$

The sources of the current density

The total parallel current density is the sum of Ohmic current and the non-inductive current:

$$\vec{j} = j_{\rm eq} + \hat{j} + \tilde{j} = j_{\Omega} + j_{\rm BS} + j_{\rm pol} + j_{\rm cd},$$

Axisymmetric and helical components of current density perturbation:

$$\hat{j} + \tilde{j} = \underbrace{(-j_{\rm eq} + \hat{j}_{\Omega} + \hat{j}_{\rm BS} + \hat{j}_{\rm cd})}_{n=0} + \underbrace{\tilde{j}_{\Omega} + \tilde{j}_{\rm BS} + \tilde{j}_{\rm pol} + \tilde{j}_{\rm cd}}_{n\neq 0}$$

Source term for the equations is included as $[\nabla \times \mathbf{E}_{\rm P}]$, where

$$\mathbf{E}_{\rm P} = \hat{\mathbf{E}}_{\rm P} = \eta(-j_{\rm eq} + \hat{j}_{\rm BS} + \hat{j}_{\rm cd}) \qquad \text{for} \quad n = 0$$

$$\mathbf{E}_{\rm P} = \eta(\tilde{j}_{\rm BS} + \tilde{j}_{\rm pol} + \tilde{j}_{\rm cd}) \qquad \text{for} \quad n \neq 0$$

The bootstrap current $j_{\rm BS}$ is included in the simplest model form:

$$\hat{j}_{\rm BS} = Ag \cdot 1.46\sqrt{\varepsilon}[-\frac{\partial \hat{P}/\partial\rho}{B_{\rm pol}}],$$

$$\tilde{j}_{\rm BS} = Ag \cdot 1.46\sqrt{\varepsilon}[-\frac{\partial P_{n\neq 0}/\partial\rho}{B_{\rm pol}}],$$

where $Ag = O(1)$ is the geometric parameter of the model.

The polarization current $\tilde{j}_{\rm pol}$ is included in the model form:

$$\tilde{j}_{\rm pol} = -\frac{W_{th}^2}{W^2}\tilde{j}_{\rm BS}$$

where W_{th} is the parameter of the model.

- **Representation of current density from ECCD**

Current density j_{cd} from ECCD is represented as a radially localized toroidal current

$$\mathbf{J_{cd}} = j_{cd}\mathbf{e}_{\varphi}, j_{cd} = j(\psi^{\star})$$

on the perturbed helical magnetic flux $\psi^{\star}$.

A normalized helical flux function :

$$\tilde{\psi^{\star}} = -(\rho - \rho_s)^2 \pm \frac{W_{mn}^2}{8} cos(m\theta - n\varphi + \alpha\pi)$$

represents the local behaviour near the resonant surface ρ_s.

The island width W is defined as

$$W = 4\sqrt{\frac{q_s^2 Y^1(\rho_s)}{m\rho_s q'}},$$

where $Y^1 = \sqrt{g}B^1$ and g is a metric element.

Define

$$j_{\rm cd}(\tilde{\psi^{\star}}) = I_{\rm cd}\frac{1}{2\pi^{3/2}W_{\rm cd}} e^{\tilde{\psi^{\star}}/W_{\rm cd}^2}$$

The following simplified form of $j_{\rm cd}(\tilde{\psi^{\star}})$ is used in NFTC code.

$$\mathrm{j_{cd}} = I_{\rm cd}\frac{1}{2\pi^{3/2}W_{\rm cd}} e^{-(\rho-\rho_0)^2/W_{\rm cd}^2}[1 \pm \tfrac{1}{8}(\tfrac{W_{mn}}{W_{\rm cd}})^2 \cos(m\theta - n\varphi + \alpha\pi)]$$

Parameters:

- $I_{\rm cd}(t\|W)$ is the total ECCD current.This can have any arbitrary dependence on time. A square wave is used in the simulations presented here.

- $W_{\rm cd}$ is the width of radial distribution,
- $\Delta\rho = \rho_0 - \rho_s$ denotes the offset of the driven current layer from the rational surface.
- $\Phi(t) = \alpha\pi$ is the phase fitted to the magnetic island rotation.

- **Modification of the transport equations**

$$\frac{\partial P}{\partial t} = \cdots + \nabla_\perp \cdot (\chi_\perp \nabla_\perp P) + \nabla_\parallel \cdot (\chi_\parallel \nabla_\parallel P);$$
$$\frac{\partial \hat{P}}{\partial t} = \cdots + \nabla_\perp \cdot (\chi_\perp \nabla_\perp \hat{P}) + \nabla_\parallel \cdot (\chi_\parallel \nabla_\parallel \hat{P}) + [\nabla_\parallel \cdot (\chi_\parallel \nabla_\parallel P)]_{n=0} + Q;$$

The unit vector along magnetic field line is defined as :

$$\mathbf{b}_{\rm tot} \equiv \frac{\mathbf{B}_{\rm tot}}{|\mathbf{B}_{\rm tot}|} \cong \frac{\mathbf{B}_{\rm eq} + \hat{\mathbf{B}} + \mathbf{B}}{|\mathbf{B}_{\rm eq}|} \equiv \mathbf{b}_{\rm eq} + \hat{\mathbf{b}} + \mathbf{b}.$$

The differential operator along magnetic field line is:

$$\nabla_\parallel P_{\rm tot} = (\mathbf{b}_{\rm tot} \cdot \nabla) P_{\rm tot} = (\mathbf{b}_{\rm eq} \cdot \nabla + \hat{\mathbf{b}} \cdot \nabla + \mathbf{b} \cdot \nabla)(P_{\rm eq} + \hat{P} + P)$$

The total heat conductivity operator is:

$$\begin{aligned}
\nabla_\parallel^2 P_{\rm tot}\big|_{n\neq 0} &= \underline{\mathbf{b}_{\rm eq} \cdot \nabla (\mathbf{b}_{\rm eq} \cdot \nabla P + \mathbf{b} \cdot \nabla P_{\rm eq})} + \\
&+ \mathbf{b}_{\rm eq} \cdot \nabla (\mathbf{b} \cdot \nabla P) + \mathbf{b} \cdot \nabla (\mathbf{b}_{\rm eq} \cdot \nabla P) + \mathbf{b} \cdot \nabla (\mathbf{b} \cdot \nabla P_{\rm eq}) + \\
&+ \underline{\mathbf{b} \cdot \nabla (\mathbf{b} \cdot \nabla P)} + \\
&+ [\hat{\mathbf{b}} \cdot \nabla (\mathbf{b}_{\rm eq} \cdot \nabla P + \mathbf{b} \cdot \nabla P_{\rm eq}) + \mathbf{b} \cdot \nabla (\mathbf{b}_{\rm eq} \cdot \nabla \hat{P} + \hat{\mathbf{b}} \cdot \nabla P_{\rm eq}) + \\
&+ \mathbf{b}_{\rm eq} \cdot \nabla (\hat{\mathbf{b}} \cdot \nabla P) + \mathbf{b}_{\rm eq} \cdot \nabla (\mathbf{b} \cdot \nabla \hat{P}) + \\
&+ \hat{\mathbf{b}} \cdot \nabla (\mathbf{b} \cdot \nabla P) + \mathbf{b} \cdot \nabla (\hat{\mathbf{b}} \cdot \nabla \hat{P} + \hat{\mathbf{b}} \cdot \nabla P + \mathbf{b} \cdot \nabla \hat{P}) + \\
&+ \hat{\mathbf{b}} \cdot \nabla (\hat{\mathbf{b}} \cdot \nabla P + \mathbf{b} \cdot \nabla \hat{P})];
\end{aligned}$$

$$\nabla_\parallel^2 P_{\rm tot}\big|_{n=0} = \mathbf{b}_{\rm eq} \cdot \nabla (\mathbf{b} \cdot \nabla P) + \mathbf{b} \cdot \nabla (\mathbf{b}_{\rm eq} \cdot \nabla P) + \mathbf{b} \cdot \nabla (\mathbf{b} \cdot \nabla P_{\rm eq});$$

$$\nabla_\parallel^2 \hat{P}\Big|_{n=0} = (\mathbf{b}_{\rm eq} + \hat{\mathbf{b}}) \cdot \nabla ((\mathbf{b}_{\rm eq} + \hat{\mathbf{b}}) \cdot \nabla \hat{P}).$$

Underlined terms in the cylindrical approximation:

$$\nabla_\parallel^2 P_m\big|_{n\neq 0} \cos(m\theta - n\varphi) = \left\{ \frac{1}{|\mathbf{B}_{\rm eq}|^2} \left[-F^2 P + F P'_{\rm eq} \frac{1}{\sqrt{g}} Y^1 \right] + \right.$$
$$\left. + \left[Y^1 \frac{1}{\sqrt{g}} \frac{\partial}{\partial \rho} \left(\frac{1}{|\mathbf{B}_{\rm eq}|^2} \frac{Y^1}{\sqrt{g}} \frac{\partial P}{\partial \rho} \right) \right] \right\}_{mn} \cos(m\theta - n\varphi); \; F_{mn} = -B^3_{\rm eq} \left(\frac{m}{q} - n \right).$$

ADVANCED TOKAMAK DISCHARGE IN DIII–D
(AT DURATION ENDED BY 2/1 TEARING MODE)
SHOT 99411 BT(set) = –1.60 T

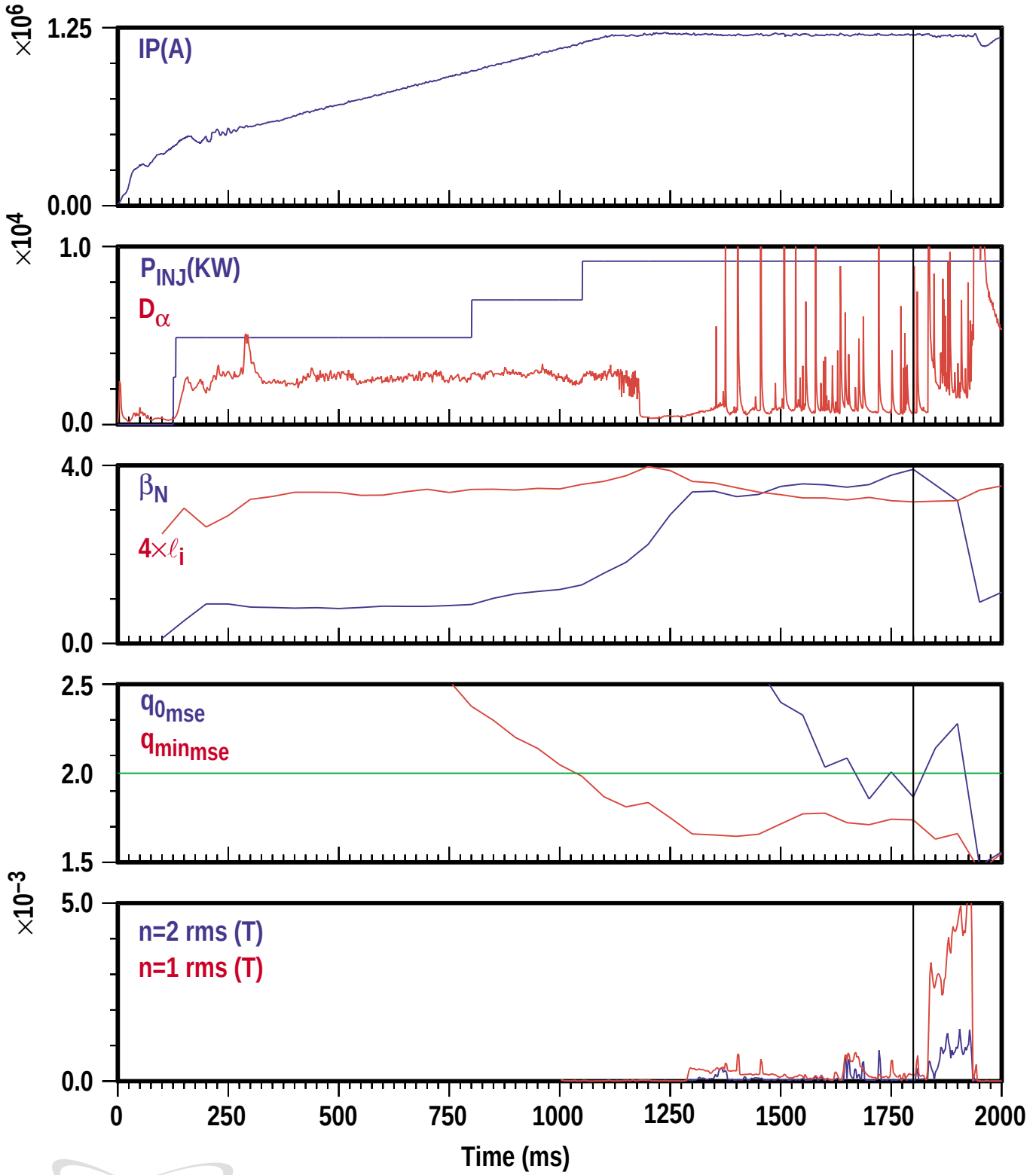

DIII–D NATIONAL FUSION FACILITY SAN DIEGO

282-00/jy

Helical magnetic perturbations in # 99411 discharge .

- First splash at t=1300ms after $q_{min} \sim 2.0$ and $\beta_N \sim 3.0$
- Second low level splash when q_0 decreases to the value 2.0.
- The third, basic splash at t=1800ms. Perturbation increases by 20 times.$\beta_N = 3.78; q_{min} = 1.67$.

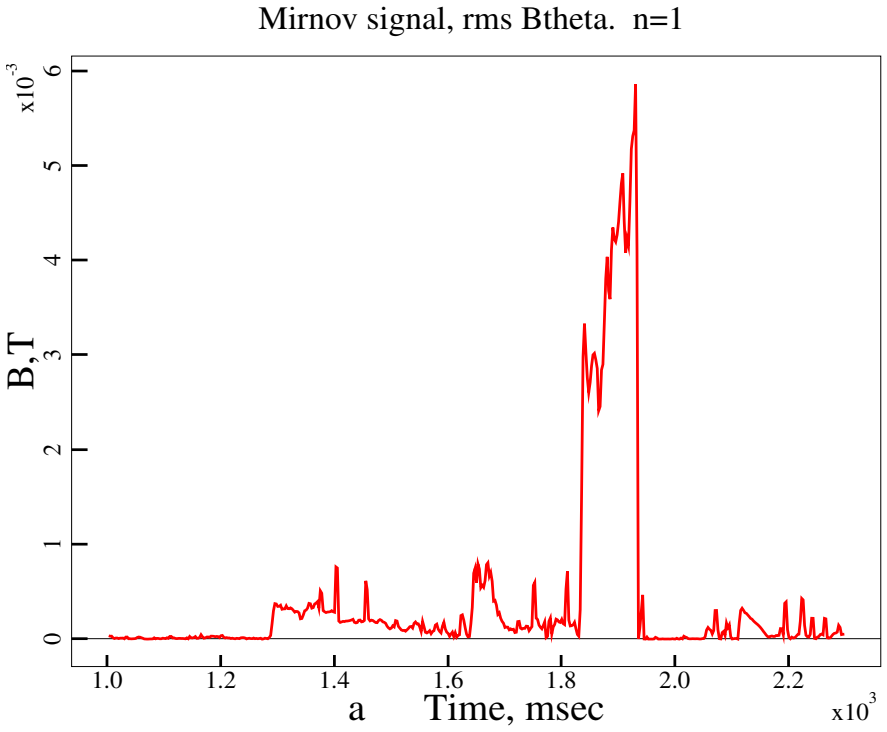

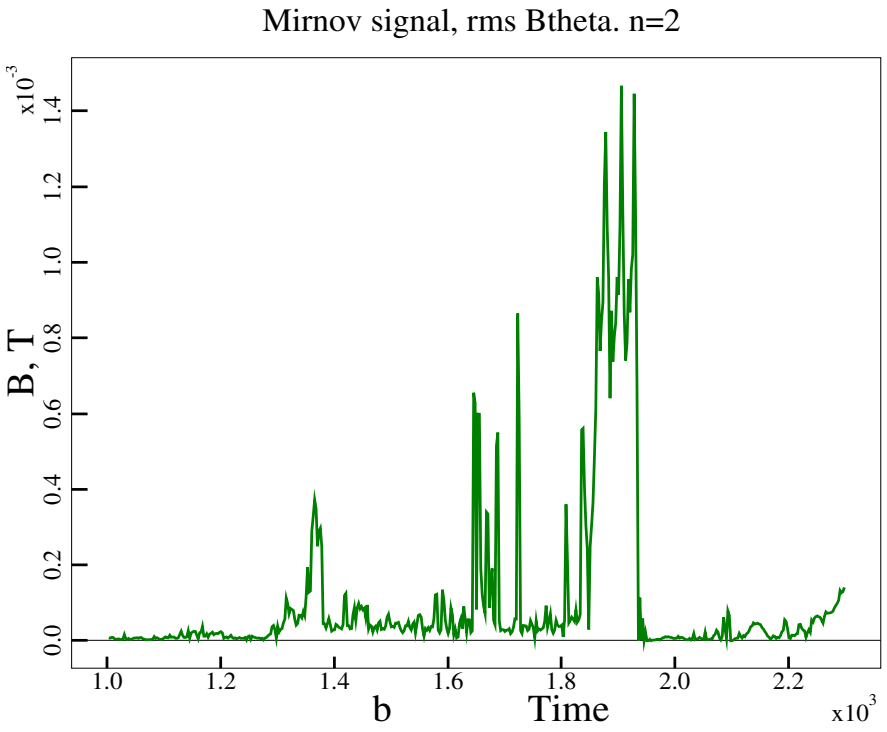

Equilibrium radial profiles in # 99411 discharge.

- At t=1800ms only one rational surface q=2 located on $\rho_s = 0.74 a_H$ and $\Delta q = q_0 - q_{min} = 0.13$, Shear S=1.28.
- At t=1915ms two rational surfaces located on $\rho_s^1 = 0.42$ and $\rho_s^2 = 0.68. S^{(1)} = -0.16, S^{(2)} = 0.43$.

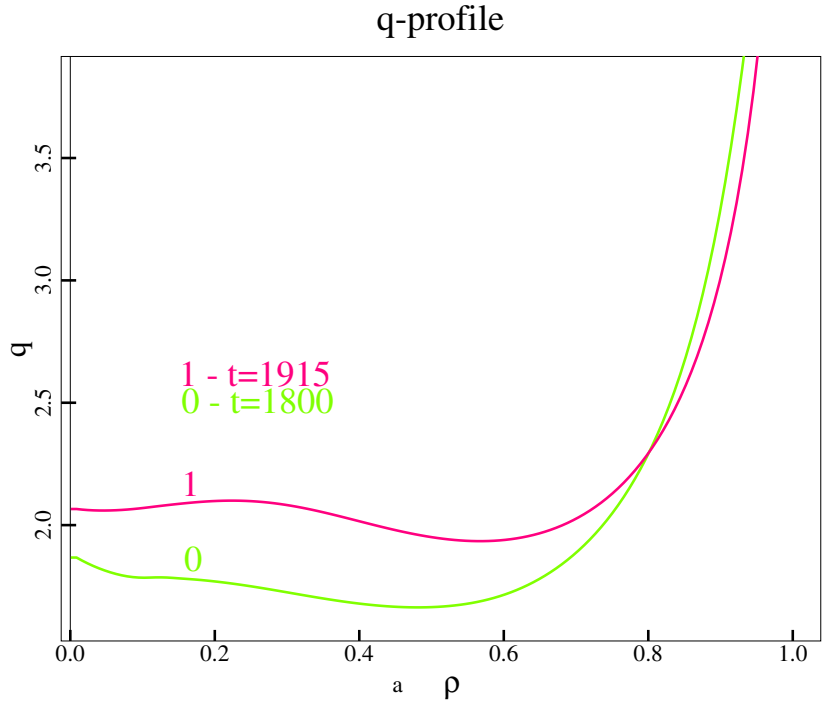

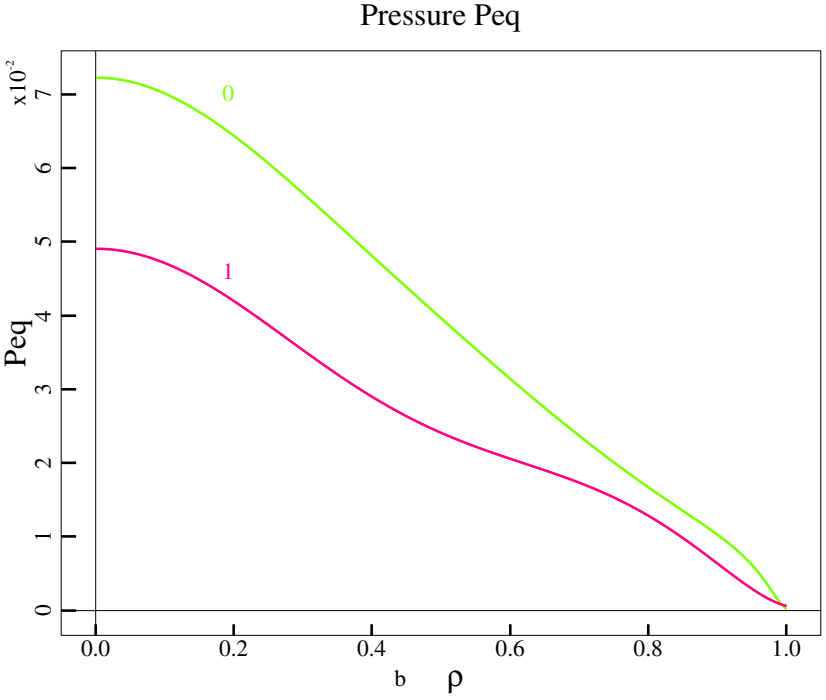

Nonlinear calculations of NTM for eq.1800ms .

- Find W_{th} for m/n=2/1 as amplitude of j_{pol} with "Eq.1.8s".
- Two parameters of the model: Ampl and W_{th} with $W_d = 0$.
  - First, increase Ampl · eigefunction (with $W_{th} = 0$ until NTM is exited. Ampl, W_{th}.
  -Second, with fixed W_{cr} change W_{th} until W(t), W_{sat} saturation will be found.
- Then found $\frac{W_{th}}{a} = 0.0235$ and this is used for all equilibriua.
- $\frac{W_{cr}}{a} = 0.045$ and $\frac{W_{sat}}{a} = 0.2$

Islands evolution , Eq.1800 msec, qmin=1.67

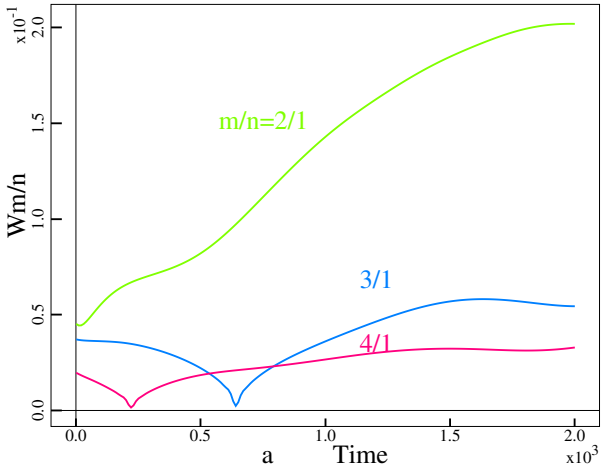

(dW,W)-Diagram

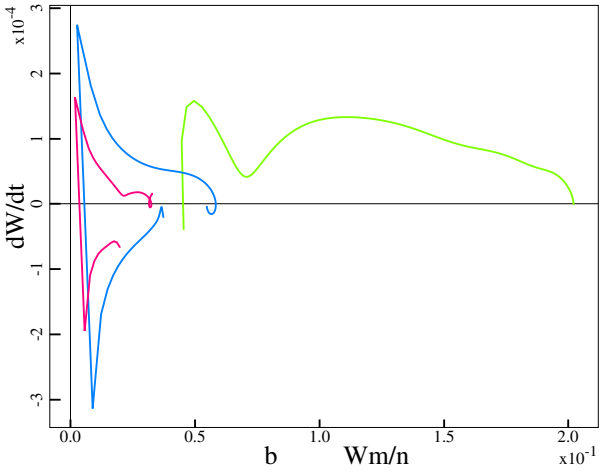

Jbs Evolution t=1800

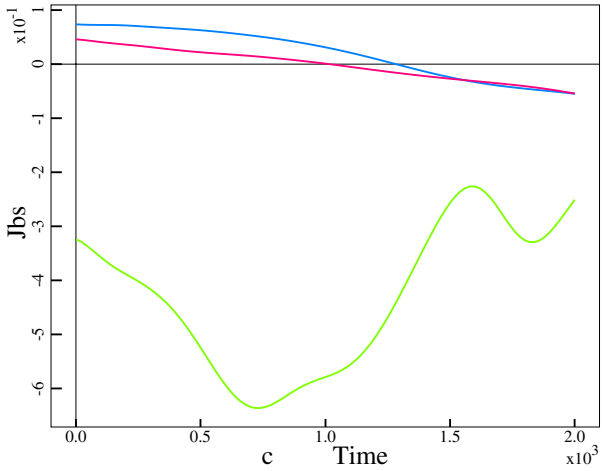

Time evolution of nonlinear solution.

- Helical perturbations of magnetic field $\rho \cdot B^{\rho}(\rho, t)$ and pressure $P(\rho, t)$ for m/n=2/1.
- Axisimmetric component of quasilinear corrections for poloidal field and pressure.
- Profiles alter from green to red

Time evolution of Y1s(2/1) profile(Eq.1800)

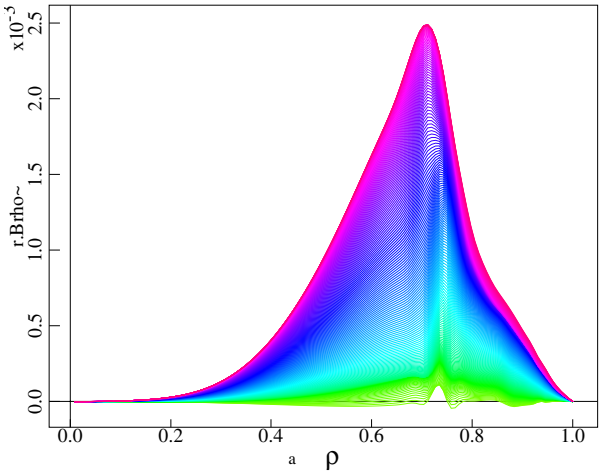

Pol.magn.field Y2^(m=0) qmin=1.67

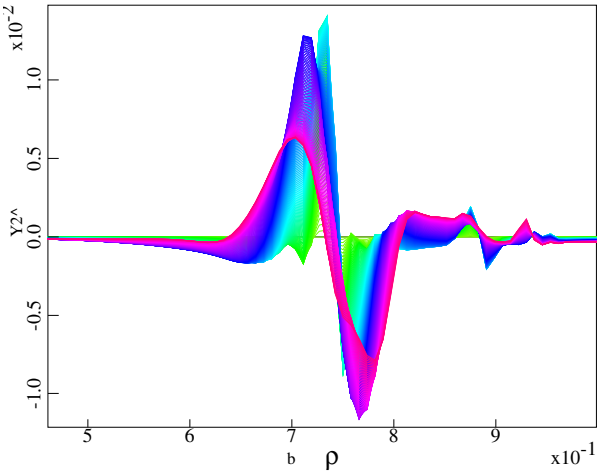

Helical pressure Pc(2/1)

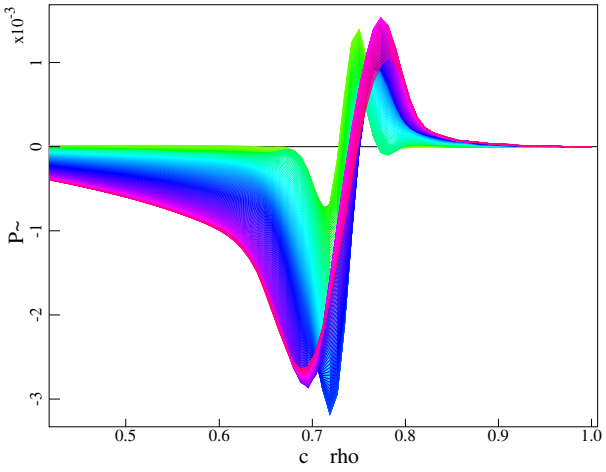

Pressure. Quasilinear corr.P^(m=0)

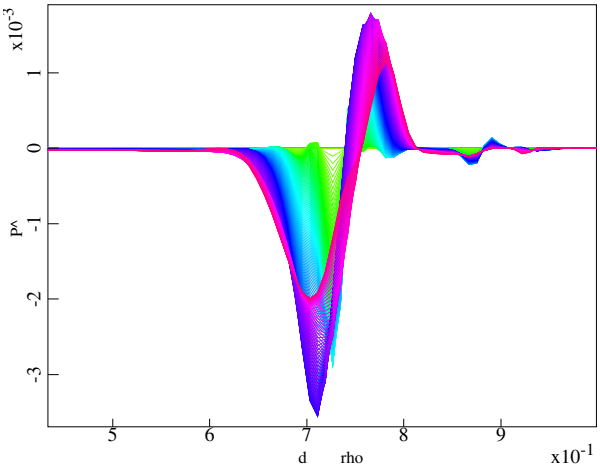

Critical island width evaluation.

- Magnetic islands m/n=2/1 evolution with different seed islands for eq.1.8s.
- Bootstrap current density for m/n=2/1 in the fixed radial point.

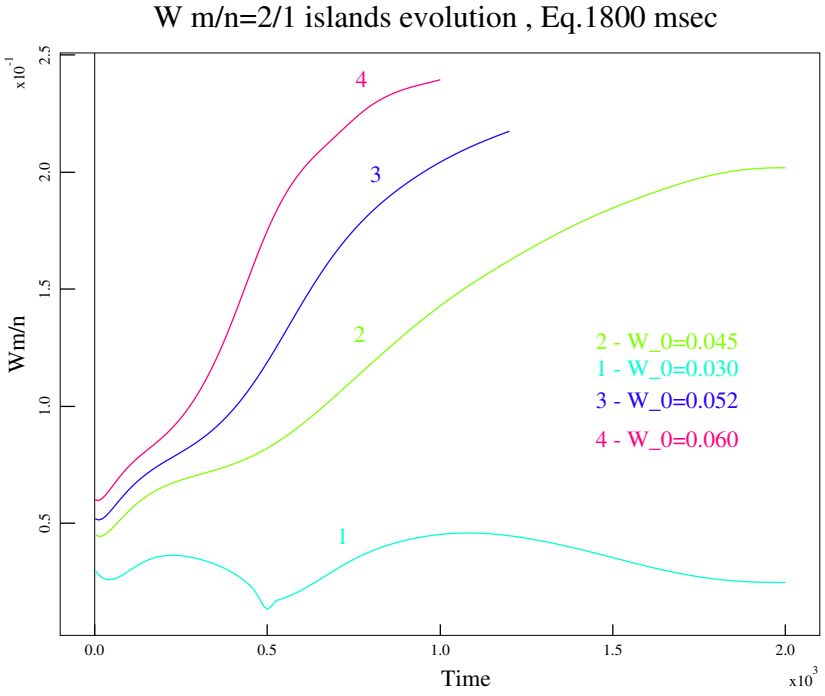

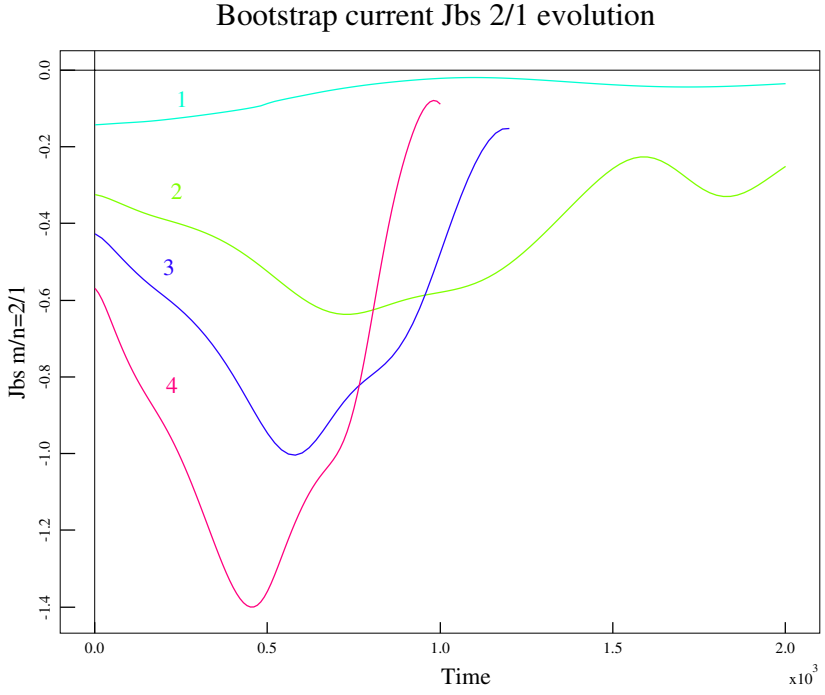

Time evolution of basic harmonics in nonlinear solution.

- m/n=2/1 NTM instability excites toroidal modes n=2 with same helicity.
- Harmonic m/m=4/2 increases to the level $W_{4/2} \sim 0.09 a_H$ and m/n=6/3 has $W_{6/3} \sim 0.07 a_H$.
- The double NTM 5/3 has the large island width $W^1_{5/3} = 0.1 a_H$ and $W^2_{5/3} = 0.07 a_H$ located in the middle of plasma area with low shear on q=5/3. Low toroidal coupling with 2/1.

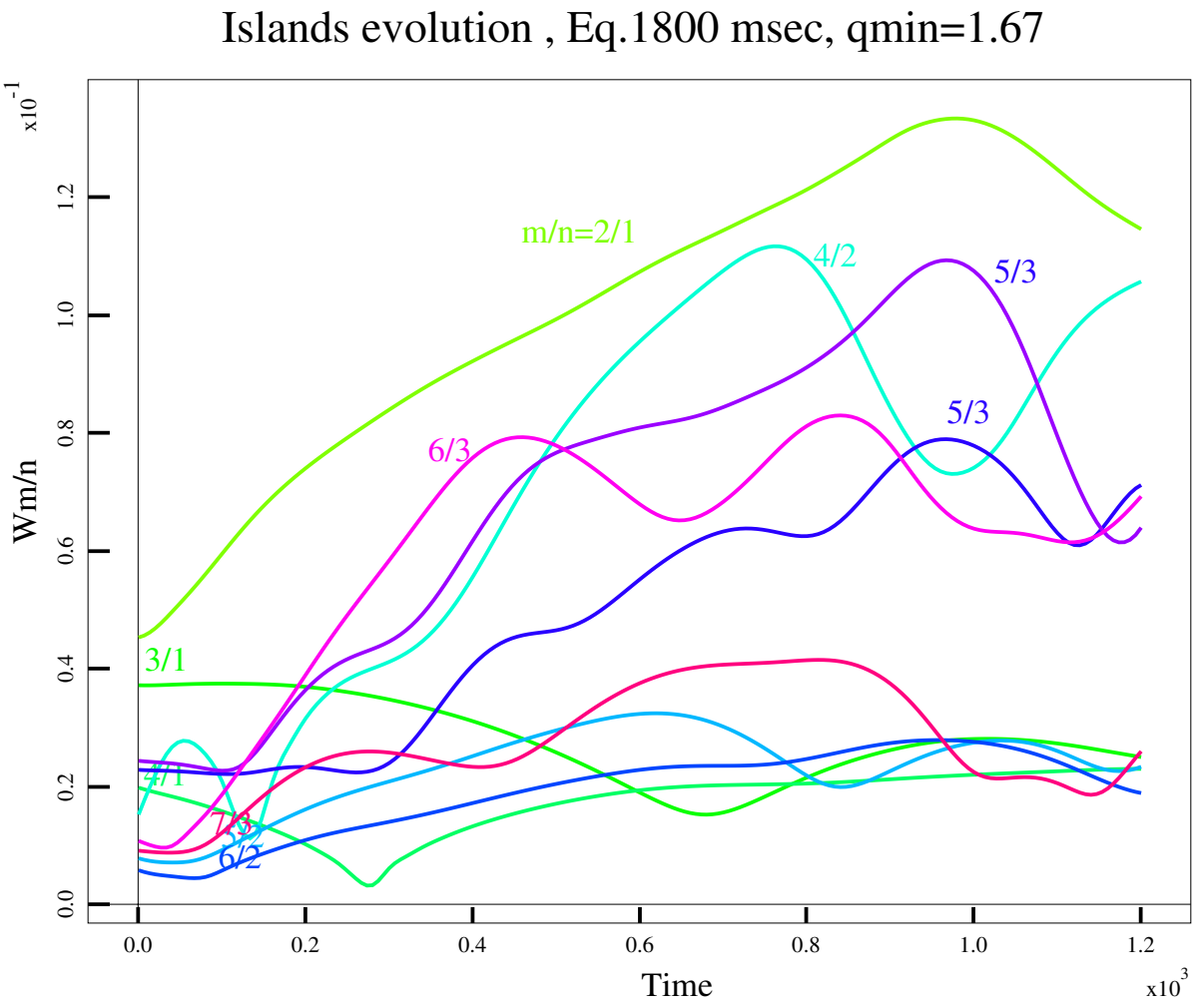

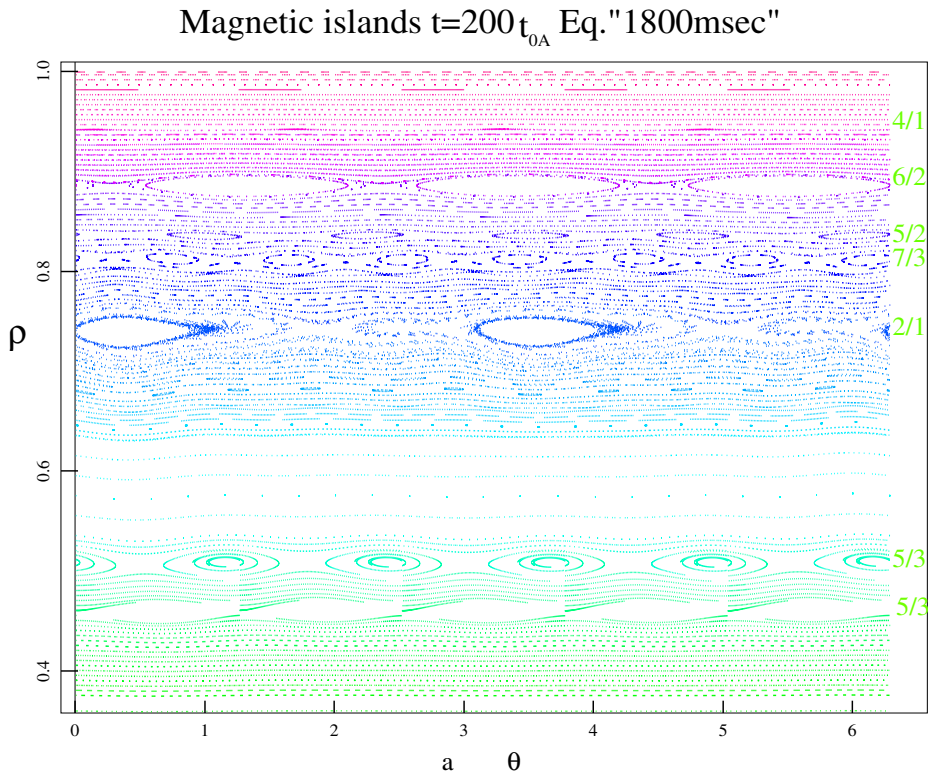
Magnetic islands t=200 t0A Eq."1800msec"
ρ
a θ
4/1
6/2
5/2
7/3
2/1
5/3
5/3
1.0
0.8
0.6
0.4
0
1
2
3
4
5
6

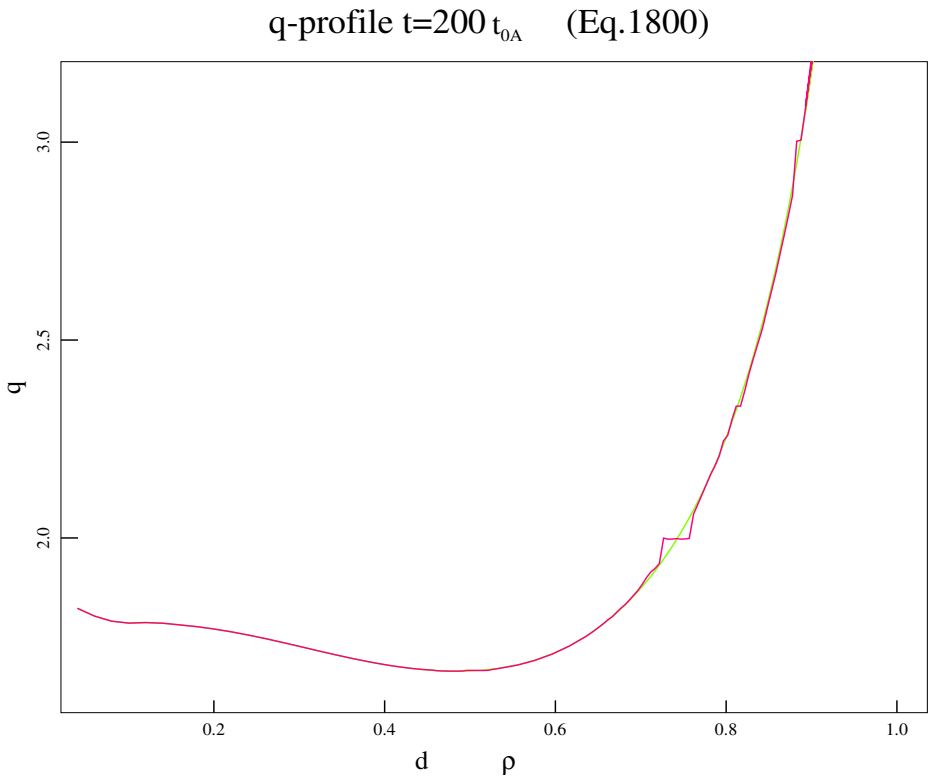
q-profile t=200 t0A (Eq.1800)
q
d ρ
3.0
2.5
2.0
0.2
0.4
0.6
0.8
1.0

Magnetic islands t=600t_{0A} Eq."1800msec"

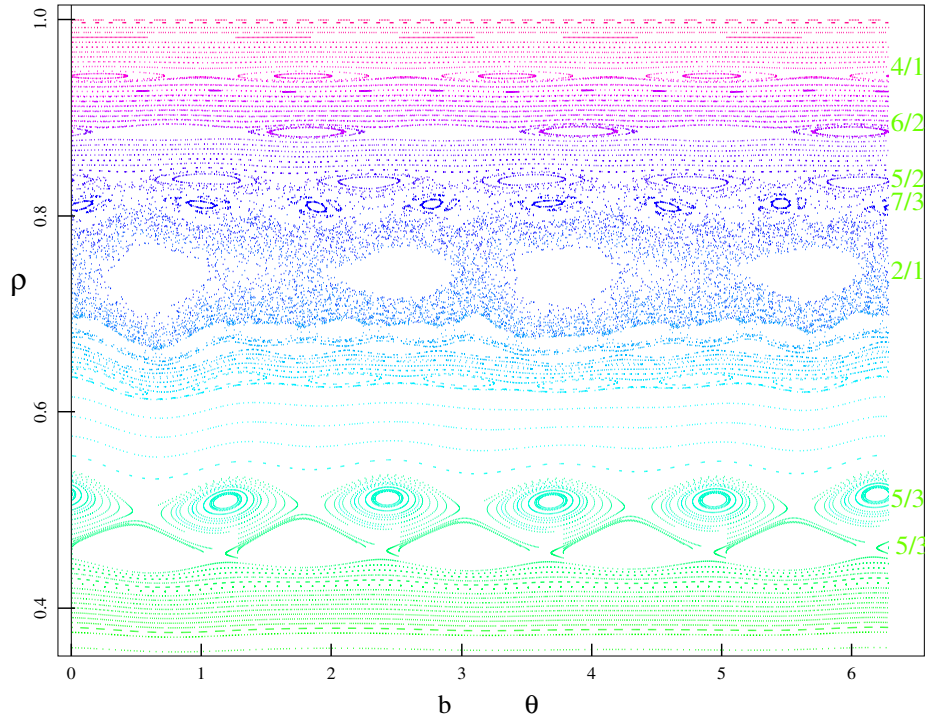

q-profile t=600t_{0A} (Eq.1800)

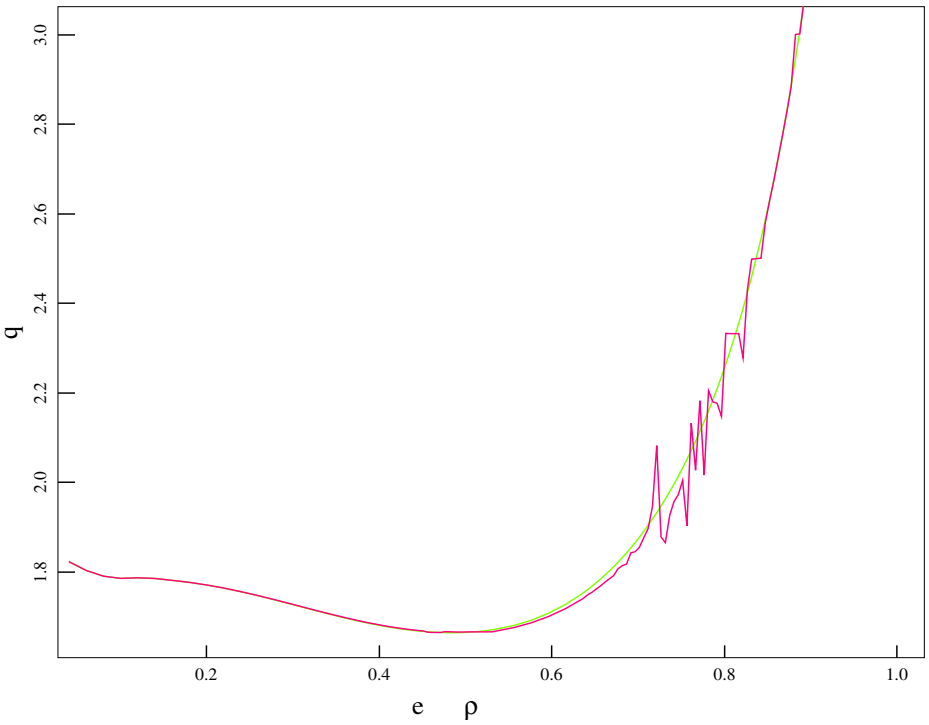

Magnetic islands t=1200t_{0A} Eq."1800msec"

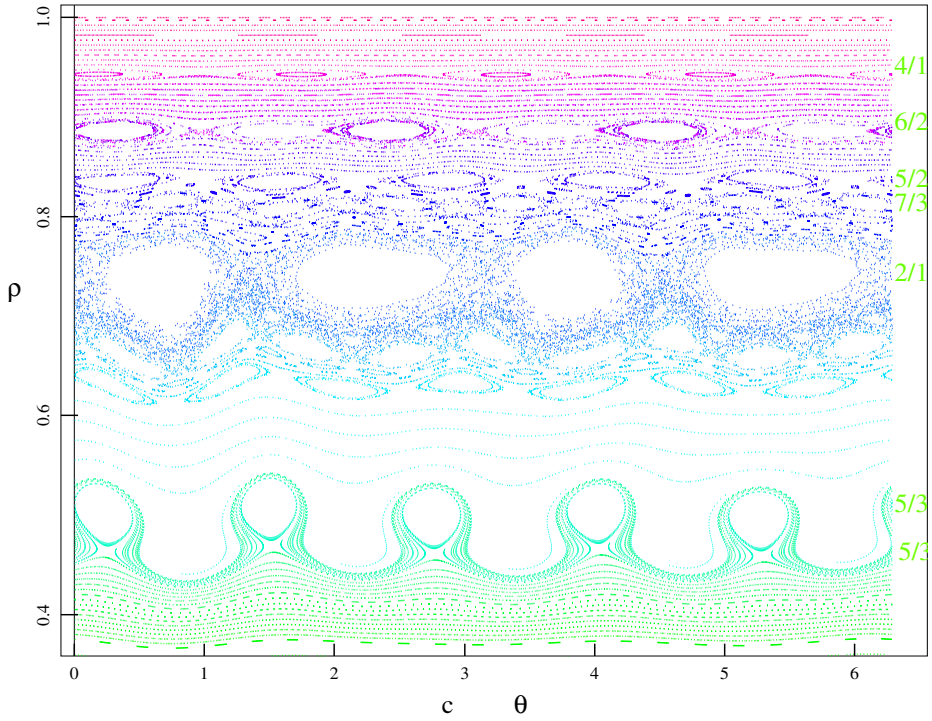

q-profile t=1200t_{0A} (Eq.1800)

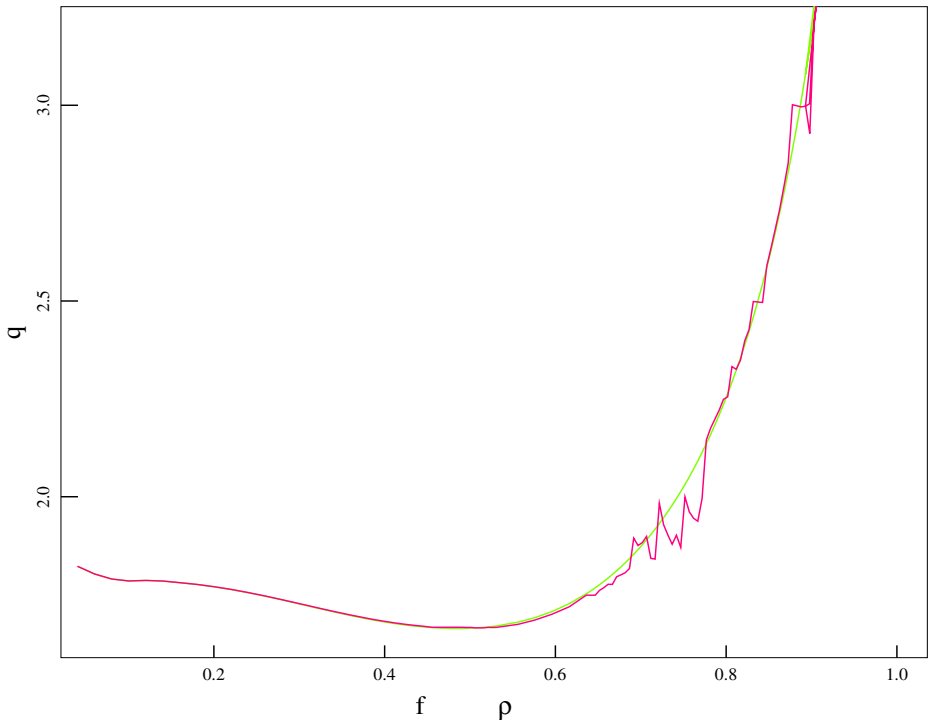

Comparison of NTM calculations with experiment .

- Amplitude of magnetic perturbation n=1 and magnetic island width $W_{2/1}$ as a function of time.
- The m/n=2/1 harmonic dominates in magnetic perturbation.
- The level and radial profile of quasilinear correction of equilibrium poloidal magnetic field Eq.1.8s corresponds to MSE diagnostic.

Comparison with experiment.Signal on Mirnov coils Bp.

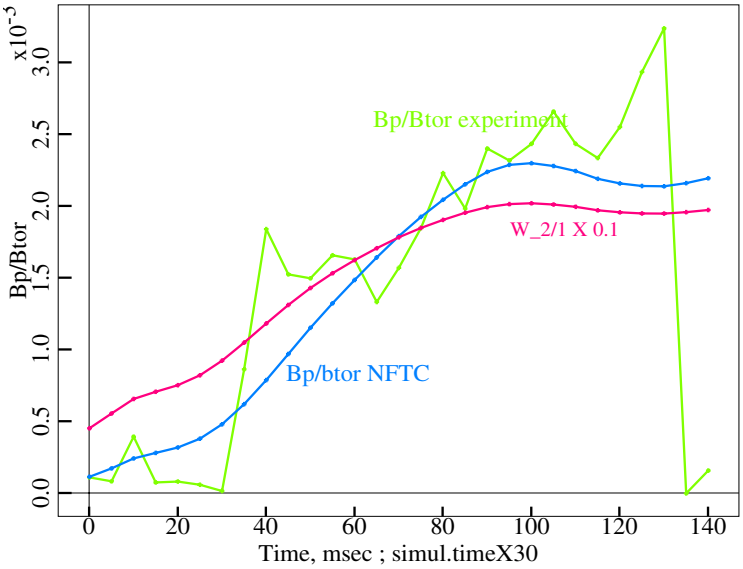

Comparison with MSE diagnostic.t=1.80-1.84s.

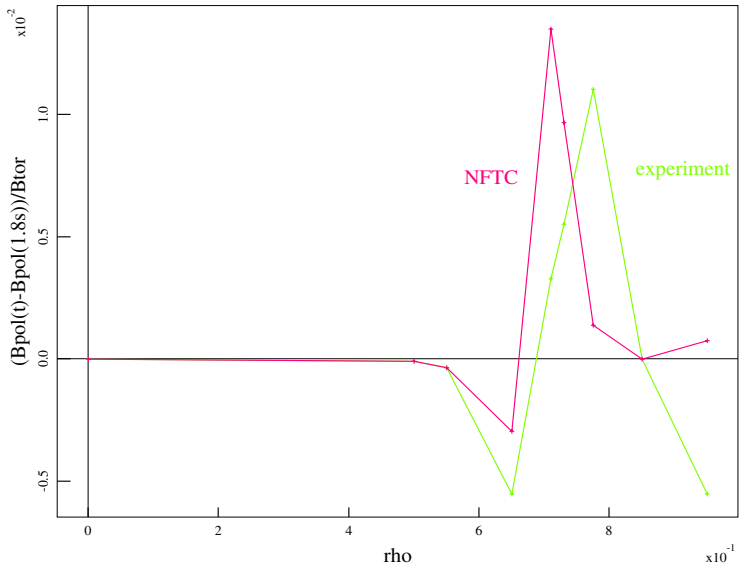

Conventional double tearing instability when q_{min} crosses 2.0 .

- Succsesive changes of eigenfunctions for decreasing q_{min}.
- When $q_0 = 2.25$ ($q_{min} = 1.993$) and $q_0 = 2.2$ ($q_{min} = 1.95$) conventional double tearing mode 2/1 is weakly unstable . Corresponds to t=1300ms in discharge.Nonlinearly stabilizes.
- When $q_0 = 1.87$($q_{min} = 1.67$) conventional tearing mode is stable.Nonlinear NTM unstable . Corresponds to t=1800ms in discharge.

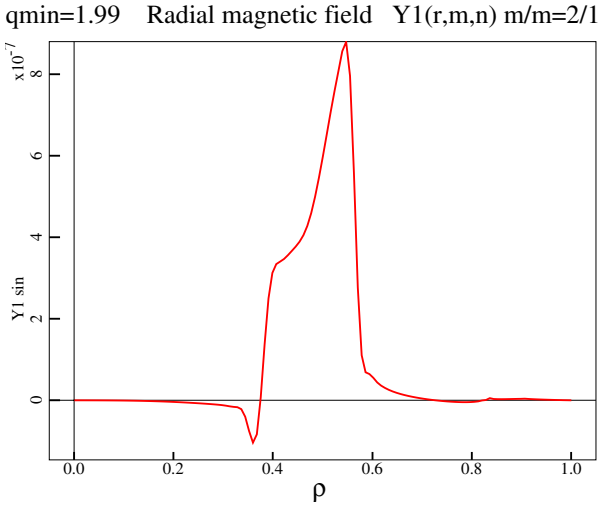

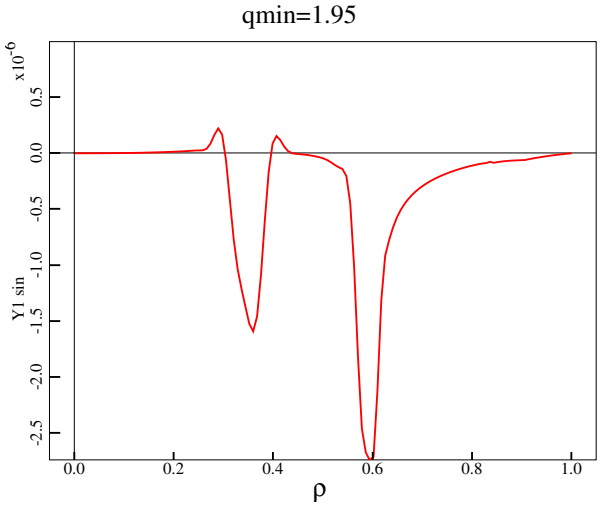

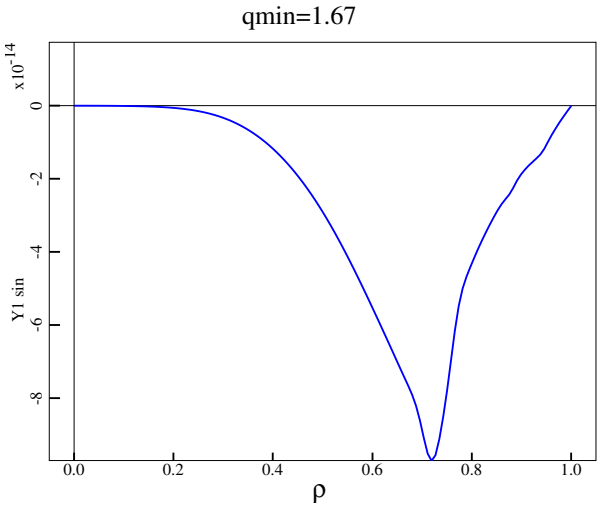

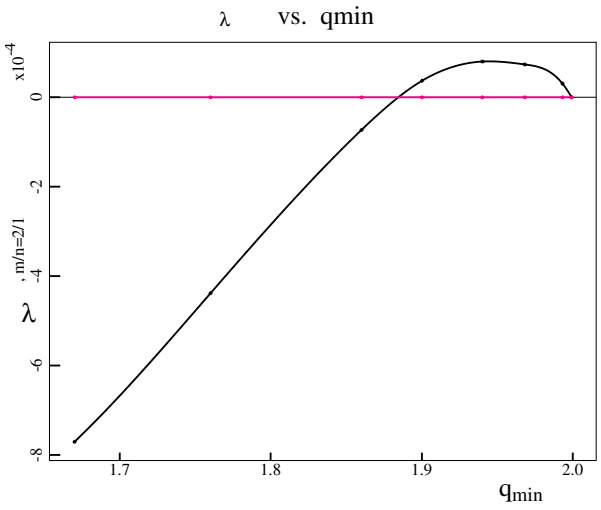

β_N limit due to NTM instability.

- Comparison of theoretical limit $\beta_N^{cr} = C \cdot \sqrt{S}$ with experimental data for # 99411 discharge.
- Equilibrium profiles and papameters are fitted to the moment t=1.8s in experiment.Linear approximation of $q_{min}(t) = 2.075 - 0.225t$ in the period of instability.
- When t=1.3 parameter $q_0 = 2.0$ and $q_{min} = 1.78$ the first MHD burst happens. When t=1.8 the main NTM instability is excited.

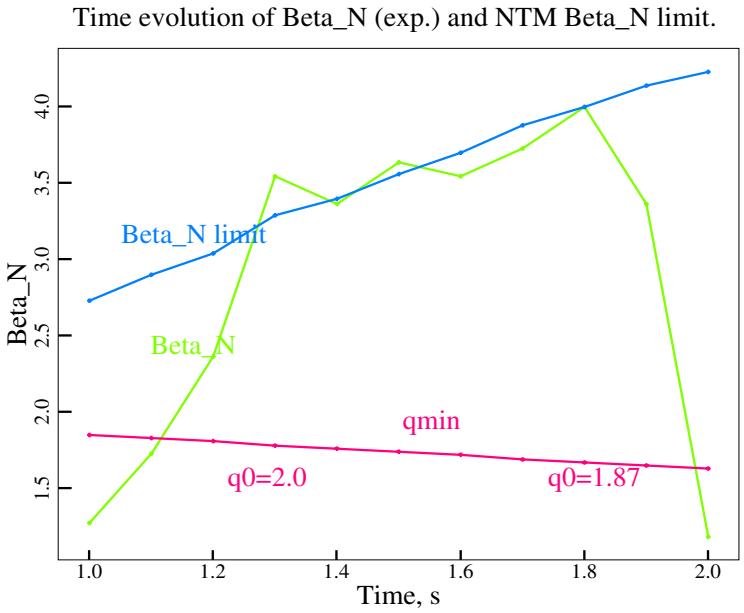

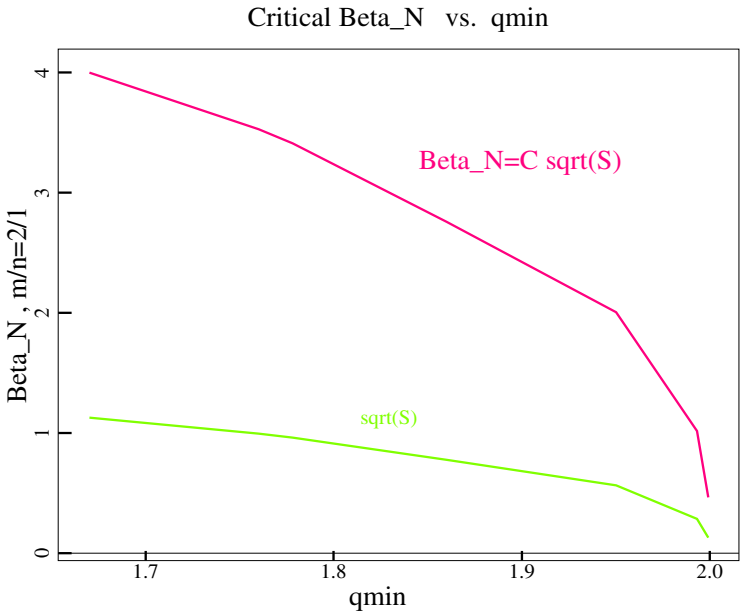

Decreasing of central pressure due to NTM instability .

- Time evolution of quasilinear correction of equilibrium pressure profile shows the decreasing of central pressure due to NTM instability.
- Heat conductivity is artificially increased by two orders in the area of magnetic islands overlapping.(4/2,6/3,5/3,..).

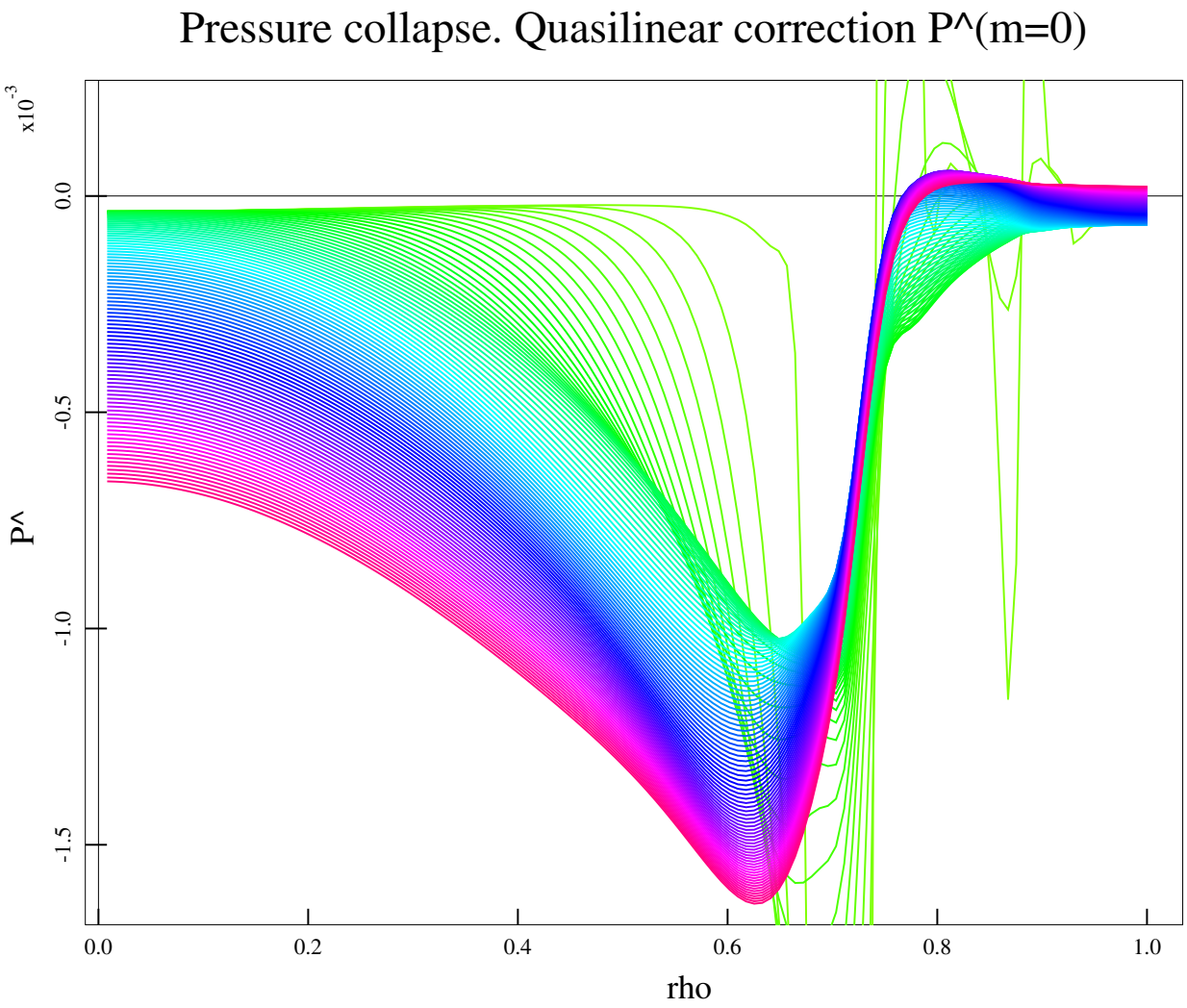

Magnitude of ECCD current needed for NTM suppression.

- a) W(t) with different magnitude of Icd/Ip. $W_{cd} = 0.06a_H$. Island width begin to oscilate. Critical seed island $W^{cr}_{2/1} = 0.045a_H$. If $I_{cd}/I_p > 0.055$ then $W_{sat} = W_{max} = 0.02a_H$.
- b) $W^{sat}_{2/1}$ and $W^{max}_{2/1}$ vs. Icd/Ip.

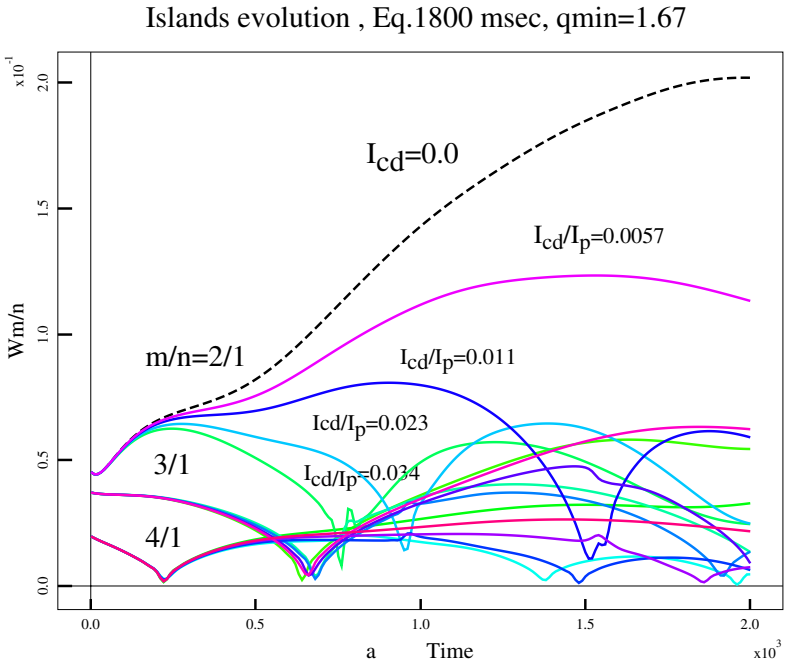

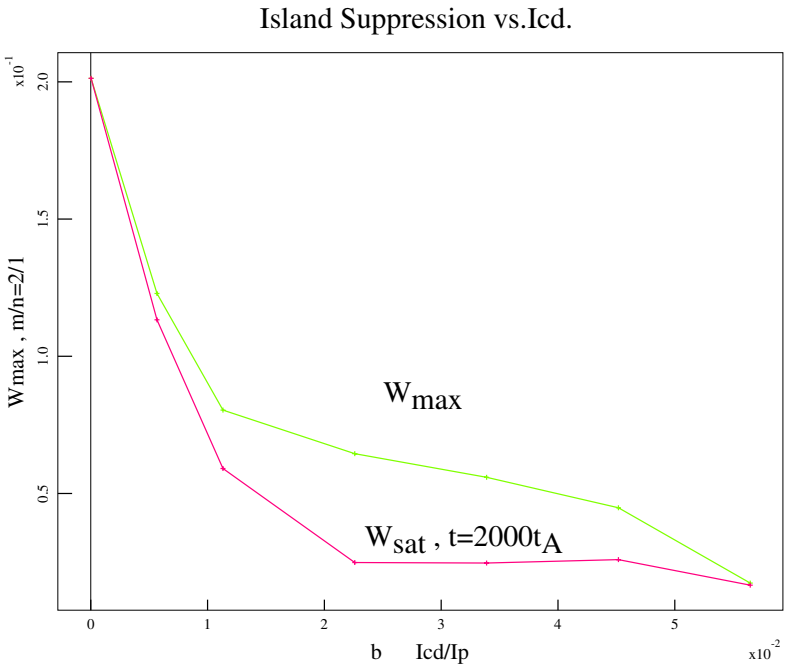

The effect of driven current layer width Wcd .

- The effectiveness of magnetic islands suppression increases with decreasing of driven current layer Wcd, when the magnitude of Icd/Ip is constant (here 0.023).
- The less Wcd the less period of oscillations. $W_{max} \approx W_{cd}$. The best conditions: if $W_{cd} > 0.5 W^{cr}_{seed}$ then no oscillations during period of suppression.

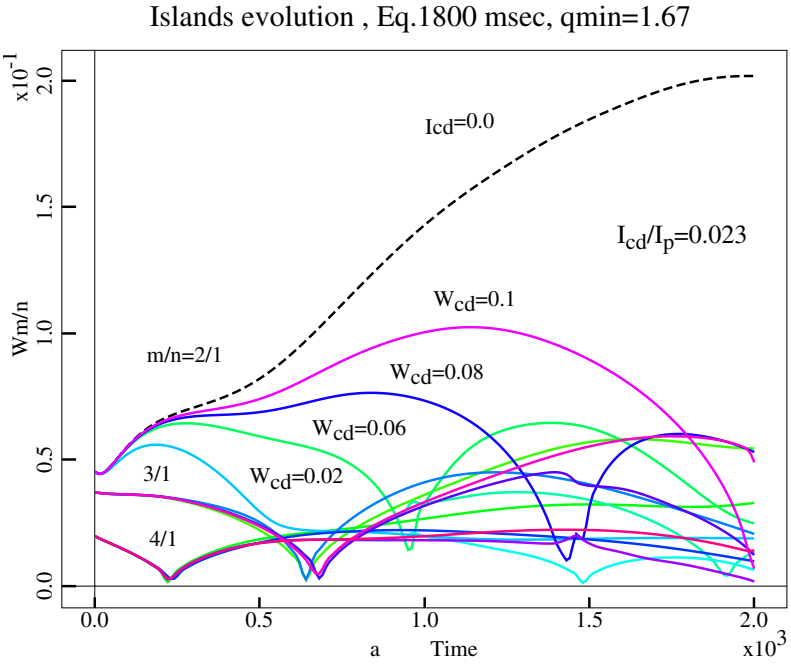

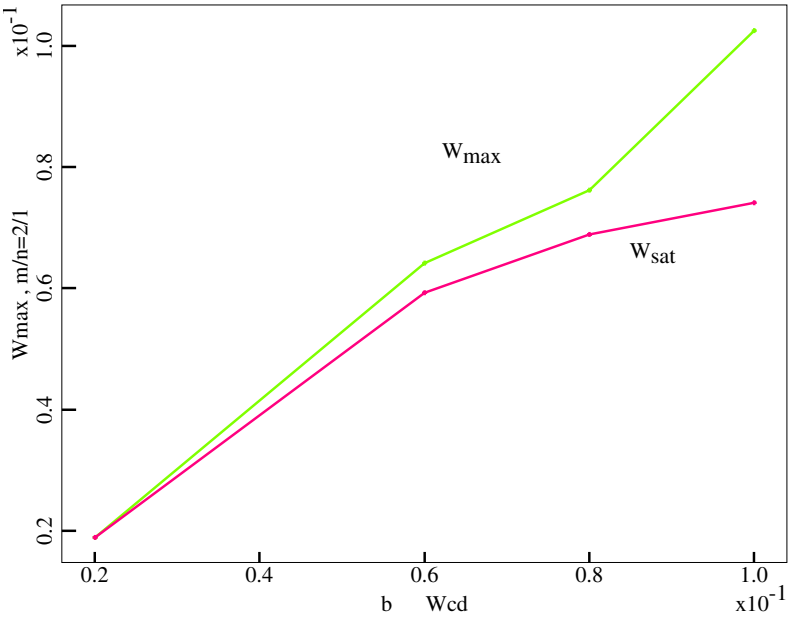

The effectiveness of magnetic islands suppression.

- Area of magnetic islands suppression on the planes: $(I_{cd}/I_p; W_{cd}/a_H)$ and $(I_{cd}/I_p; W/W_{cd})$.
- Each point on curves corresponds to the same maximal magnetic islands width equal $W_{2/1} = 0.06 a_H$ obtained during calculations.

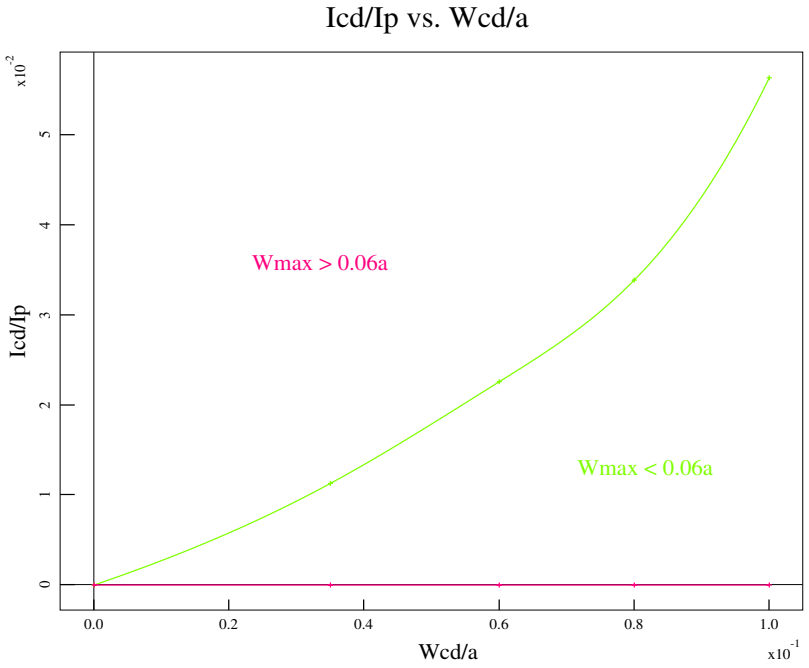

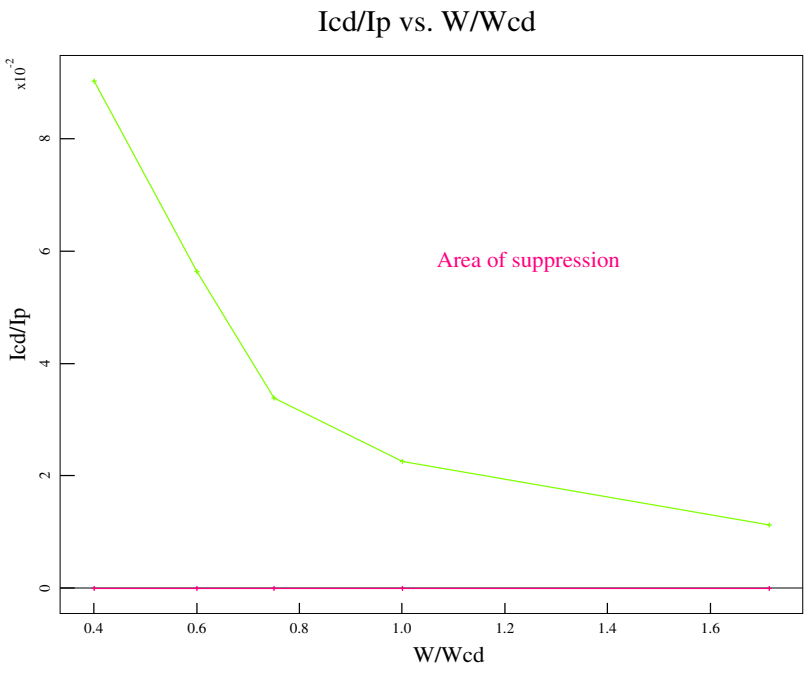

The effect of max(Jcd) Location

- Maximum of stabilization effect occurs when $\Delta\rho = 0$.When $\Delta\rho \geq W_{cd}/a_H$, then the stabilization effect is lost.$Wcd = 0.06a_H$ for these cases.

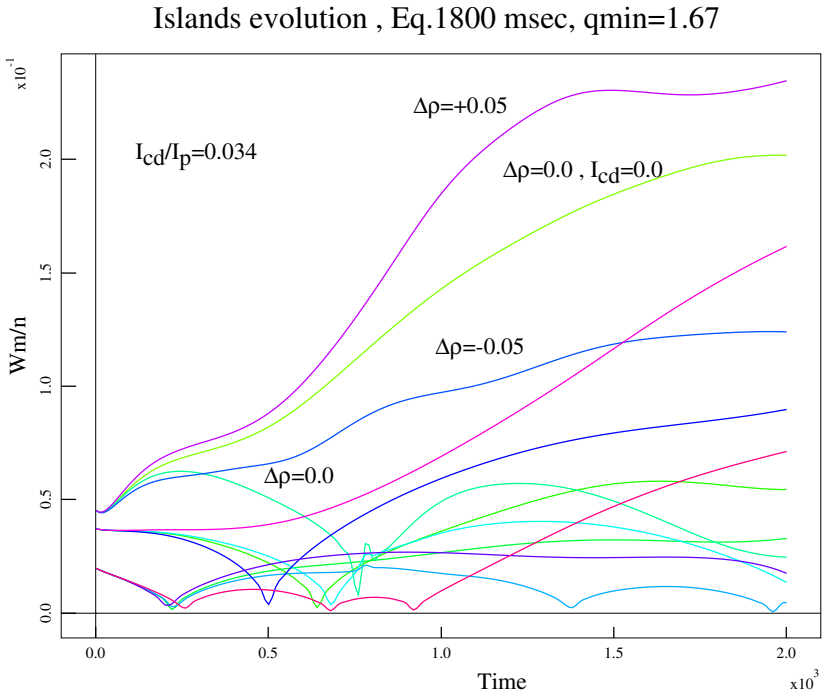

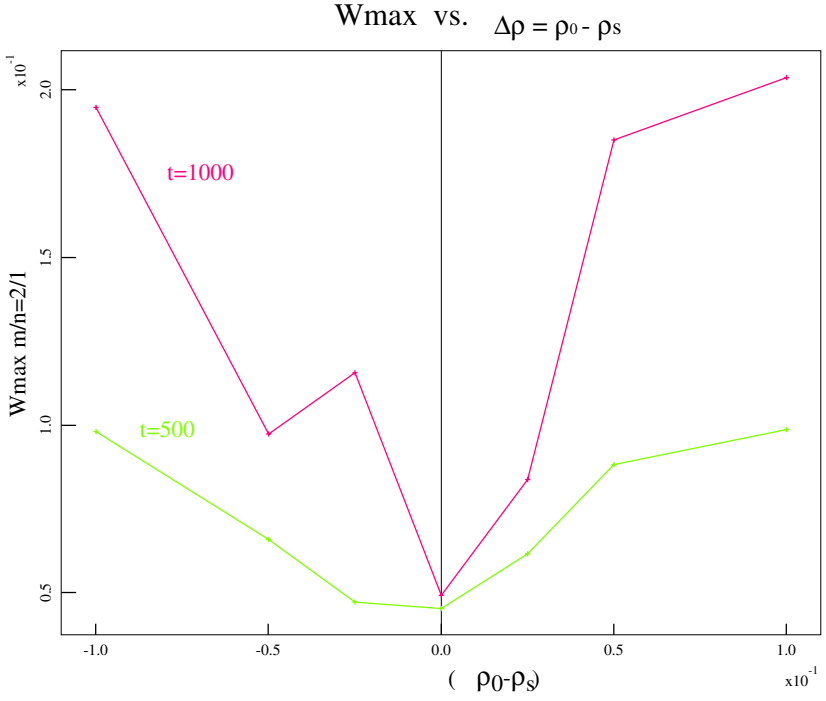

ECCD suppression vs. islands rotation .

- Magnetic islands width during ECCD suppression with different islands rotation.
- Comparison of ECCD efficiency for only axi-symmetric component and axi-symmetric and helical components of j_{cd}.

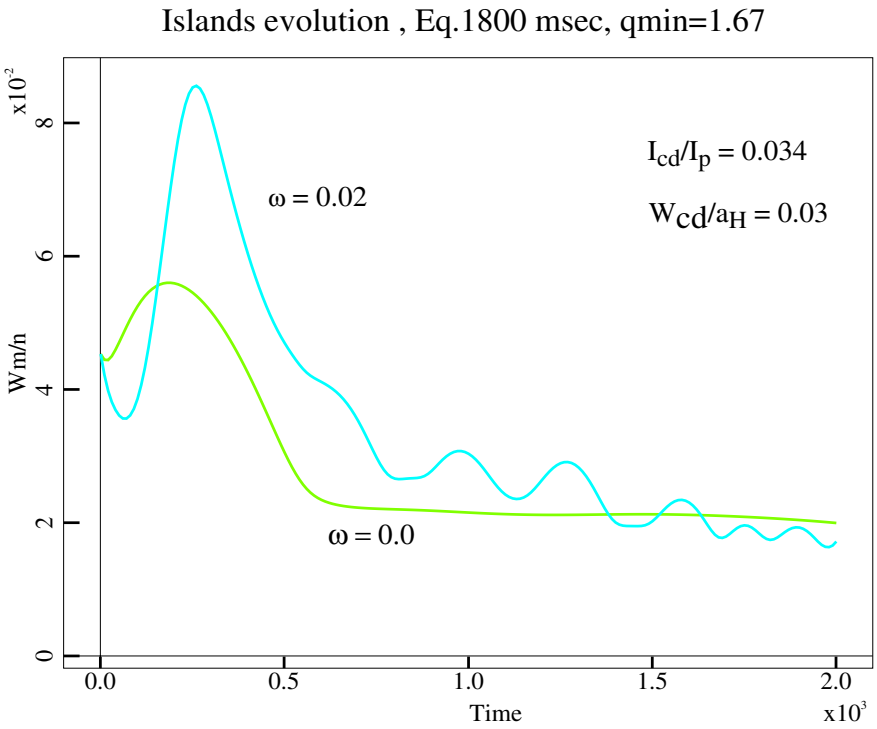

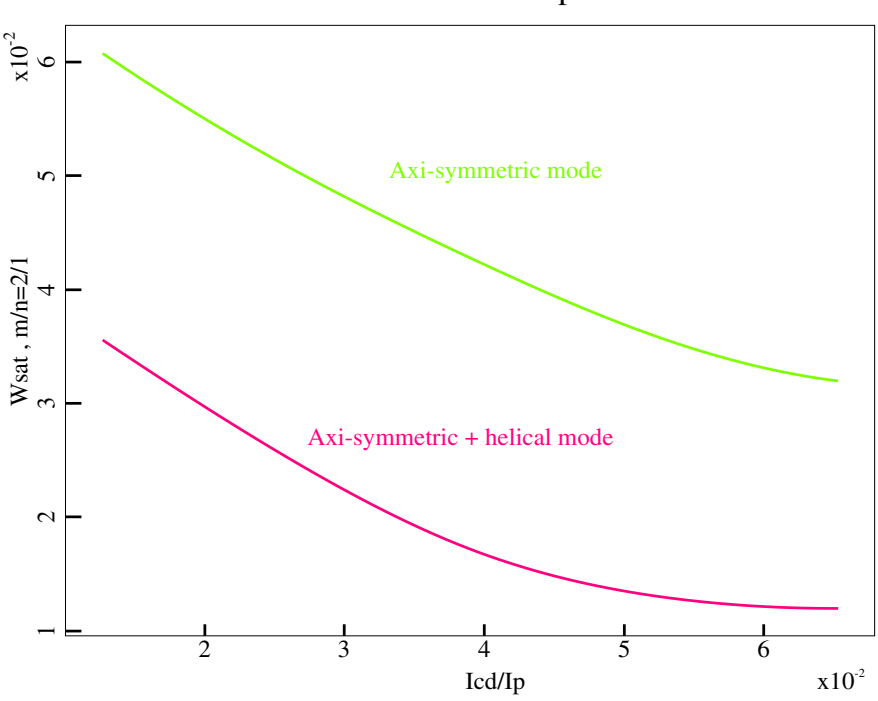

CONCLUSIONS

- Stability calculations by NFTC of high $\beta_N \star H$ AT in DIII-D (# 99411 discharge) were performed.
  Comparison of nonlinear NTM calculations with experimental data shows
  - correspondence with the level of the helical magnetic perturbations with Mirnov signal
  - correspondence of quasilinear correction of equilibrium poloidal field with MSE diagnostic.

- Explanation of critical seed island were done as aftereffect of conventional tearing instability when q_{min} crosses the value $q_{min} = 2$.

- A radially localized current from ECCD is included for NFTC code as a source term. Driven current j_{cd} depends on perturbed magnetic surfaces and has helical and axisymmetric components in its representation. Self-consistent calculations using the NFTC code show the effectiveness of ECCD suppression of neoclassically destabilized magnetic islands.

- ECCD current which is needed for the island suppression increases parabolically with the driven current layer width W_{cd}
  The less W_{cd} is , the less total current is needed for suppression. Magnetic island can be suppressed to the level of order W_{cd}. For $W_{cd} < 0.05 a_H$ and $I_{cd} = 0.05 I_p$ the seed magnetic islands are suppressed and NTM stabilizes at t=1800ms in discharge # 99411.

- Localization of $max(j_{cd})$ relating rational surface of mode is very important fro stabilization. Maximum shift is of order $\Delta\rho_{max} \sim W_{cd}/a_H$, which is equal to $0.05 a_H$ for # 99411 discharge.